Visual
Abstract

Deep Learning algorithm for the assessment of the first damage initiation monitoring the energy release of materials

Dario Santonocito, Dario Milone
University of Messina, Italy
dsantonocito@unime.it, http://orcid.org/0000-0002-9709-9638
dmilone@unime.it, http://orcid.org/0000-0001-8140-7571

ABSTRACT. Monitoring the energy release during fatigue tests of common engineering materials has been shown to give relevant information on fatigue properties, reducing the testing time and material consumption.

During a static tensile test, it is possible to assess two distinct phases: In the first phase (Phase I), where all the crystals are elastically stressed, the temperature trend follows the linear thermoelastic law; while, in the second phase (Phase II), some crystals begin to deform, and the temperature assumes a non-linear trend. The macroscopic transition stress between Phase I and Phase II could be related to the "limit stress" that, if cyclically applied, would lead to material failure. Nowadays, it is impossible to distinguish the transition between Phase I and Phase II in an objective way. Indeed, it is up to the operator's experiences.

This work aims to create a universal methodology that predicts the limit stress by assessing the change in temperature trend by adopting Neural Networks. A Deep Learning algorithm has been created and trained on experimental data coming from static tensile tests performed on several classes of materials (steels, plastics, composite materials). Once trained, the network can predict the transition temperature at which the first plastic deformation occurs within the material.

KEYWORDS. Fatigue limit; STM; Deep learning; Infrared thermography.

OPEN ACCESS

INTRODUCTION

I n the past thirty years, infrared thermography has found wide application during fatigue testing of different materials [1–5] . Indeed, fatigue is a dissipative phenomenon in which a large part of mechanical work provided to the specimen is dissipated into heat [6].

The first researcher who applied infrared thermography to assess the damage evolution was Risitano [7] in 1984. In 2000, La Rosa and Risitano [8] proposed a method that identifies the fatigue limit of a sample by monitoring its superficial temperature, i.e. the Thermographic Method (TM, or Risitano's Thermographic Method). Risitano and co-workers [9] proposed a lean protocol to obtain the S-N curve of the materials by adopting a minimal number of specimens.

By monitoring the superficial temperature of a specimen subjected to a uniaxial tensile test, Clienti et al. [10] observed a deviation from the linear trend, due to the thermoelastic law, of the temperature signal. The corresponding macroscopic stress was correlated to a stress level, the so called "limit stress", that introduces in the material irreversible damage and microplasticity. Risitano and Risitano [11] proposed the Static Thermographic Method (STM) as an innovative test solution able to obtain, with a simple static tensile test, the first damage initiation in the material thanks to the observation of the superficial temperature signal. If the limit stress, assessed by the STM, is applied in a cyclical way to the specimens it would reach fatigue failure. The assessment of the limit stress has been performed by making the linear regression of the linear part (Phase I) and plateau region (Phase II) of the temperature trend; based on the ability of the operator to recognize the different phases of the temperature signal [12,13]

However, Machine Learning (ML) algorithms can be a useful aid to automatically assess the value of the limit stress by analysing the time vs temperature vs applied stress signal obtained during a static tensile test. Within the ML algorithms, Time Series Forecasting (TSF) is an entry point and can be applied to many sectors, ranging from weather forecasts to trends in economic indicators [14].

Nature represents many physical systems whose interaction leads to a wide diversity of complex dynamics [15]. Recurrent neural networks (RNNs) are one the types of neural networks that analyses sequence functions. Sequences on which this kind of algorithm can work are made up of time series, videos, or images.

Long-term memory networks (LSTMs) are adopted in this work because they are a special type of RNN. From an experimental data set of static tensile tests made of time, temperature, and applied stress level of several kinds of material, the LSTM network has been trained on the operator experience to evaluate the limit stress. The accuracy of the neural network and the predicted value have been evaluated.

PHYSICAL AND THEORICAL BACKGROUND

Static Thermographic Method

Since 1986 [16] Risitano and co-workers have adopted infrared thermography to investigate the behaviour of several kinds of materials subjected to fatigue loads. If we monitor the temperature evolution during a fatigue test, performed at a given frequency f and stress ratio R, under a stress level above the fatigue limit σ_0 of the material, we can observe a trend characterized by a first temperature rise, followed by a plateau region and then a sudden increase of the temperature up to the specimen's failure [8].

By exploiting the energy release of the material during the fatigue test, the fatigue limit can be quickly identified as the stress level at which the stabilization temperature exhibits a significantly higher value than the previous applied stress level. A gradual fatigue test can also be performed, gradually increasing the applied stress, and recording the stabilization temperatures. The entire S-N curve of the material is thus obtained by adopting a limited number of specimens and in a concise time (Risitano Thermographic Method, R-TM) [9]. Over the past thirty years, RTM has been applied to different materials, from steels to composites.

In 2010, Clienti et al. [10] applied infrared thermography on specimens subject to static tensile loads. They observed how during the static test, the superficial specimen's temperature shows a decrease, due to the linear thermoelastic law by Lord Kelvin [17] For the first time, they correlated the limit stress σ_{lim}, a macroscopic damage stress for the material, at the first deviation from the linearity of the temperature decrease ΔT during the uniaxial test performed on plastics.

In 2013 Risitano and Risitano [11] proposed a methodology to evaluate the first damage inside the material by monitoring the temperature trend during a uniaxial tensile test. During a static tensile test of common engineering materials, the temperature evolution detected employing an infrared camera is characterized by three phases (Fig. 1). Firstly, an approximately linear decrease due to the thermoelastic effect (Phase I); therefore, the temperature deviates from linearity up to a minimum temperature value (Phase II), then undergoes to a higher increase until the material fails (Phase III).

Under uniaxial stress and adiabatic test conditions, Lord Kelvin's thermoelastic law can be simplified as:

$$\Delta T = K_m T_0 \sigma_m \tag{1}$$

here K_m is the thermoelastic coefficient (Pa^{-1}), T_0 is the initial specimen's temperature (K), and σ_m is the average stress in the specimen cross-section (MPa). Within the material, in the first phase (Phase I), where all the crystals are elastically stressed, the temperature trend follows the linear thermoelastic law; while, in the second phase (Phase II), some crystals are

plastically deformed, and the temperature trend deviates from the linearity as the plastic deformations are more prevalent, in correspondence of the yielding stress of the material [18,19], temperature increase up to failure.
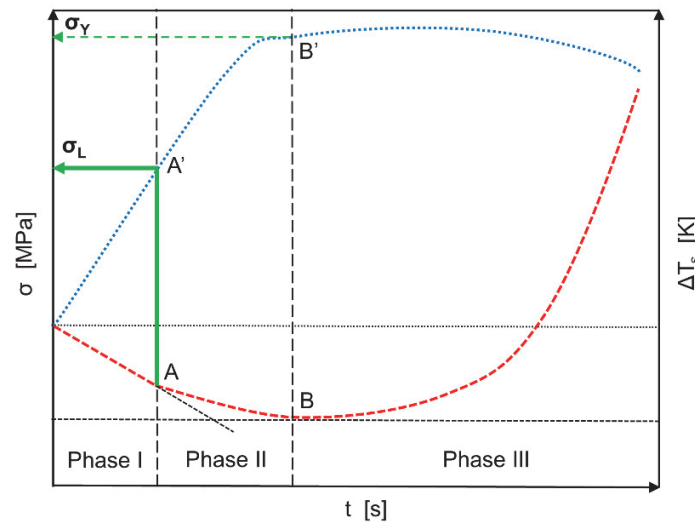

Figure 1: Qualitative ΔT_s trend vs machine time (t) vs applied stress (σ).

Important information derives from the fact that, if it is possible during a static test to estimate the stress related to the macroscopic damage at which the temperature trend loses the linearity characteristics, this stress could be correlated to a stress level that creates microscopic irreversible deformation. This critical stress is the same that, if applied cyclically to the material, will lead to fatigue failure.

Deep Learning Algorithm
A Recurrent Neural network (RNN) stores information past with which the model can predict the future characteristics of the system based on historical information. RNNs are networks made up of loops (Fig. 2) that allow keeping the information running. RNN does not start from the first information every time but from them learns from the previous phenomenon, while conventional neural networks cannot do that [20].
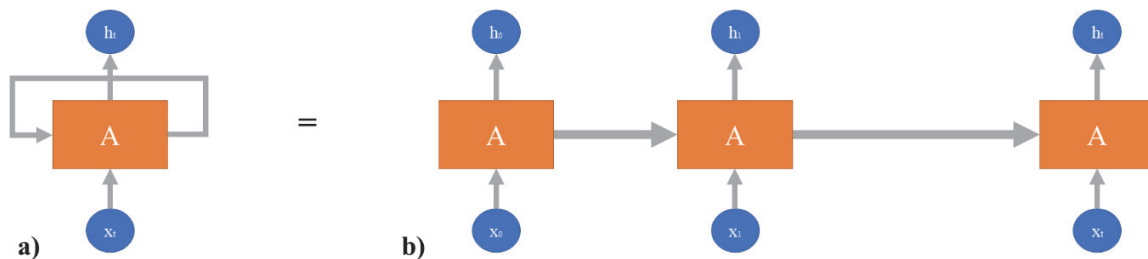

Figure 2: a) Recurrent Neural Network loop; b) Recurrent Neural Network model.

Rectangle A represents the nucleus of the neural network (hidden layer), which receives an input (x_t) and returns an output (h_t). A loop transmits the data before moving on to the next step. An RNN can be considered numerous copies of the same network, in which each time a loop is terminated, a message is passed to the following network (Fig. 2b).
Long ShortTerm Memory (LSTM) networks are the same as RNNs. The only difference is that the hidden layer updates are replaced by purpose-built memory cells [21]. The equations below represent inputs and outputs coming from the hidden layer of Fig. 3.

$$i_t = \sigma \left(W_{xi} x_t + W_{hi} h_{t-1} + W_{ci} c_{t-1} + b_i \right) \tag{2}$$

$$f_t = \sigma (W_{xf} x_t + W_{hf} h_{t-1} + W_{cf} c_{t-1} + b_f) \tag{3}$$

$$c_t = f_t c_{t-1} + i_t \tanh(W_{xc} x_t + W_{hc} h_{t-1} + b_c) \tag{4}$$

$$o_t = \sigma (W_{xo} x_t + W_{ho} h_{t-1} + W_{co} c_t + b_o) \tag{5}$$
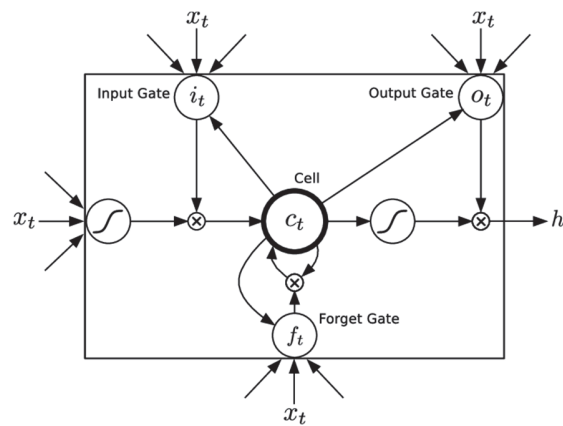
$$h_t = o_t \tanh(c_t) \tag{6}$$

Figure 3: Long ShortTerm Memory network [18].

In the figure above, σ is the logistic sigmoid function (its domain is the set of all real numbers and its range is 0÷1); i the input gate (this gate process the $h_{t-1} + x_t$ and gives out new input using the activation function which is usually Sigmoid activation function, again in the range of 0 to 1, not ignoring any information like forget gate); f the forget gate (this gate sorts out the relevant and irrelevant information and pushes forward, only the relevant information towards the cell state $h_{t-1} + x_t$). The h_{t-1} is the previous hidden state, and x_t the current input; the addition of both is processed under the sigmoid function, which will convert the output value in the range 0÷1. The "o" symbol represents the output gate; "c" the cell vectors, and "h" the hidden vectors [19].

The weight matrix controls the weights representing the influence of the input on the output. For example, W_{hi} is the hidden input gate matrix, W_{ho} is the input-output gate matrix etc. The weight matrices from the cell to the gate vectors are diagonal, so the m element in each gate vector receives input only from the elements of the vector cell. In the bidirectional LSTM, in a given time interval, it is possible to have access, in the activity of coding in sequence, to both future inputs and past inputs (Fig. 4) as proposed in [22].
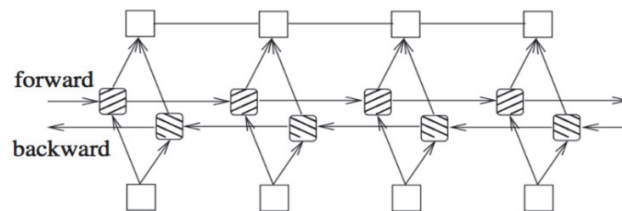

Figure 4: Bidirectional LSTM Neural Network model [22].

This uses past functionality (forward) and future functionality (backwards) for a specific period of time. The back and forth passes on the unfolded network are performed similarly to the normal back and forth network passes, except that it must uncover the hidden states for all time phases. It also takes a special processing at the beginning and at the end of the data points.

MATERIAL AND METHODS

Experimental setup

Tests to obtain data for the STM were performed on several kind of materials (steels plastics and composites), under stress or displacement control, adopting a rate to assure adiabatic conditions during the tests, i.e. the specimen must not have the time to exchange heat with the surrounding environment. Under this hypothesis, as reported by Melvin and Lucia [18,19], the "characteristic heat diffusion time" for the specimen is more and more less than the whole test time. Environmental conditions, such as room temperature, can severally affect the energy release of the material, allowing it to exchange heat with the surrounding environment by conduction and convection.

All the static tensile test under consideration were performed at the mechanical laboratory of the University of Messina. The materials under study were: stainless steel AISI 316L; medium carbon steel C45 [23]; structural steel S355 [2]; plastic composite with glass fibre PA66GF35 [24]; 3D-printed PA12 [25] and high density polyethylene HDPE-100 [26].

The typical experimental setup requires a servo-hydraulic loading machine and an infrared camera (Fig. 5). For steel specimens, an INSTRON 8854 and an MTS 810, up to 250 kN of maximum load, were adopted. For plastic and composite material, an ITALSIGMA 25 kN servo-hydraulic load machine was adopted.
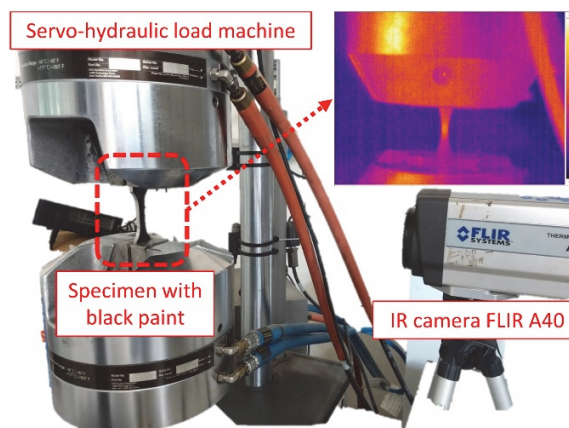

Figure 5: Experimental setup for STM.

The infrared camera FLIR A40 (thermal sensitivity of 0.08° C at 30° C) with a sample rate of 1 image per second was adopted to monitor the surface of the specimen's reduced section. The maximum temperature value has been recorded and filtered in MATLAB® with a *rlowess* filter with a data range of 5%. To enhance the thermal emissivity of the material up to 0.98, the specimen's surface was covered with a black paint.

Dataset preparation

LSTMs analyses time series forecasting problems. These problems are characterized by a single observation series; therefore, a model is needed to learn from the series of past observations to predict the next value in the sequence [27]. Before a univariate series can be modelled, it must be prepared. The LSTM model uses a function that maps a sequence of past observations as input to predict an output observation. The sequence of observations must be transformed into multiple classes that the LSTM can learn from [21].

For creating the LSTM model, a reference was made to the Python Keras library. It is a deep learning API written in Python, running on top of TensorFlow's machine learning platform. The aim of the library is to enable fast experimentation on data. The core data structures of Keras are layers and models. The simplest model type is the Sequential model, a linear stack of layers.

From the material set reported in the "Experimental setup" section, 16 static tensile tests were collected with the aim of training the neural network. A linear interpolation was adopted to scale the size of the data sets to the one of the most significant (AISI 316L, set with a number of elements equal to 1235) in order to have vector all of the same length to train the neural network.

Temperature variation on the surface of the specimen ΔT ($\Delta T = T_i – T_0$, instantaneous minus initial) during the tensile test was chosen as the variable to train the neural network.

—

A specific array structure must be adopted to provide the input for the LSTM network. The structure must include a sample (the temperature signal ΔT), the time step (sampling time from the IR camera) and a feature that the algorithm should predict. In the case studied, the character is represented by the temperature at which the signal differs from linearity even from the instant in time in which the phenomenon occurs. The feature provided as input is assessed by the intersection of the two linear regressions lines, according to the operator's experience in assessing the different temperature phases. The dimension of the input vector is 19760x2x16. The temperature signal was scaled in order to enclose the data in a range from 0 to 1(Fig. 6).
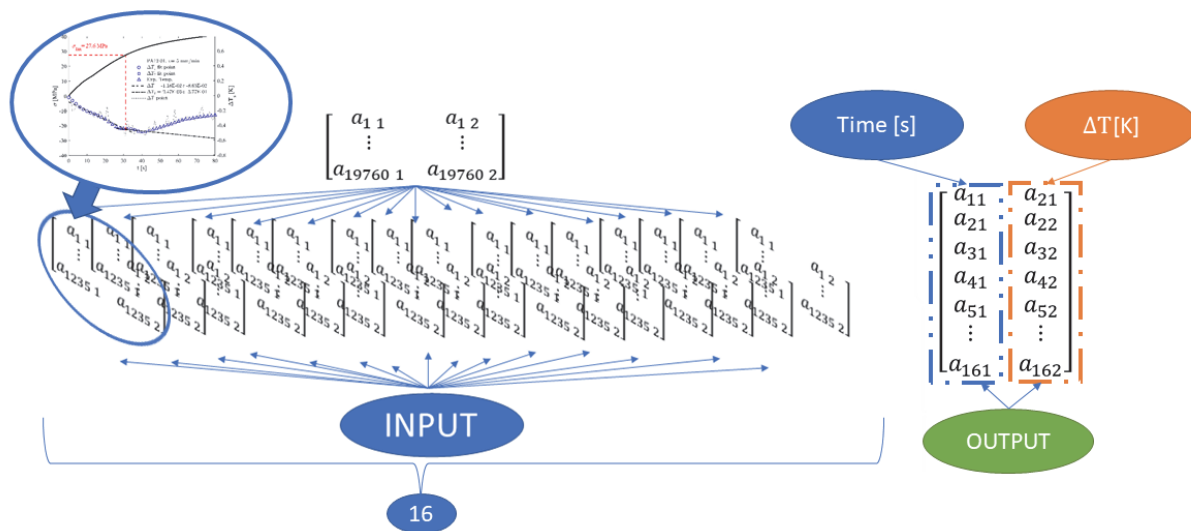

Figure 6: Features of input and output.

The collected data was divided into a set of trains and tests. The former was used to train the network, while the latter was used as feedback, in order to have a parameter of how much the algorithm returns an exact value. The test set size has been set as 20% of the total dataset size.

The adopted LSM network consists of 3 levels. To evaluate the loss, the Mean Square Error (MSE= mean square discrepancy between observed data values and predicted data values) was adopted. The output provided by the network consists of a vector composed by two columns (dimension equal to 16x2): the first represents the predicted intersection between the two straight lines, the second represents the time at which this temperature data was obtained.

RESULTS AND DISCUSSION

Accuracy of the network

The LSM network has been trained with the 80% of the whole dataset and the MSE has been evaluated. In Fig. 7, it is reported the loss (value measure of how the model being able to predict the expected outcome) vs. epochs, i.e., the mean square discrepancy value between the observed data values and the predicted data values for each iteration of the algorithm.

$$MSE = \frac{1}{N} \sum_{i=1}^{N} (y_{pred} - y_i)^2 \tag{7}$$

After a number of 1300 epochs the MSE evaluated for the train set is equal to 2.05e-5, while the MSE for the test set is to 0.067 (Fig. 7).
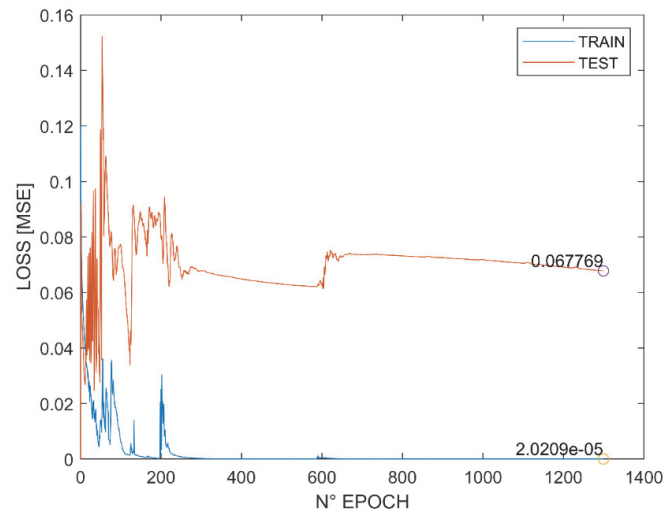
Figure 7: Loss value of the LSM network.

Further analysis has been conducted to evaluate also the RMSE (standard deviation of the residuals prediction errors). This kind of metric is adopted in a regression to assess the scatter of experimental data respect to the prediction made by the regression line:

$$RMSE = \sqrt{\sum_{i=1}^{N} \frac{1}{N}(y_{pred} - y_i)^2} \tag{8}$$

It is a measure of how the data fall around the best fit line related to training and test data. A value of 0.004 for the training data and 0.2603 for the test data have been obtained (Fig. 8).
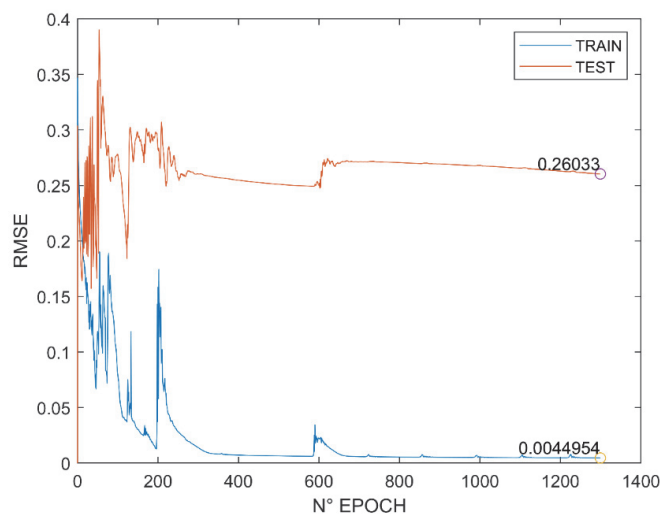

Figure 8: RMSE value of the LSM network.

Prediction of the limit stress
After analysing the parameters related to the accuracy of the network, the next step has been to make predictions on new temperature data sets to evaluate the reliability of the network in predicting the limit stress of the material. For the test

section, steel (AISI 316L), composite (PA66GF35) and plastic (PE100) materials have been chosen. The outputs from the analysis have been named as:

    1) Expected value: value obtained from the analysis of an expert operator.
    2) Predicted value: value obtained from the neural network.

Fig. 9, Fig. 10, and Fig. 11 are reported to better visualize the outputs coming from the algorithm. The results of the train, test and validate dataset are shown below.
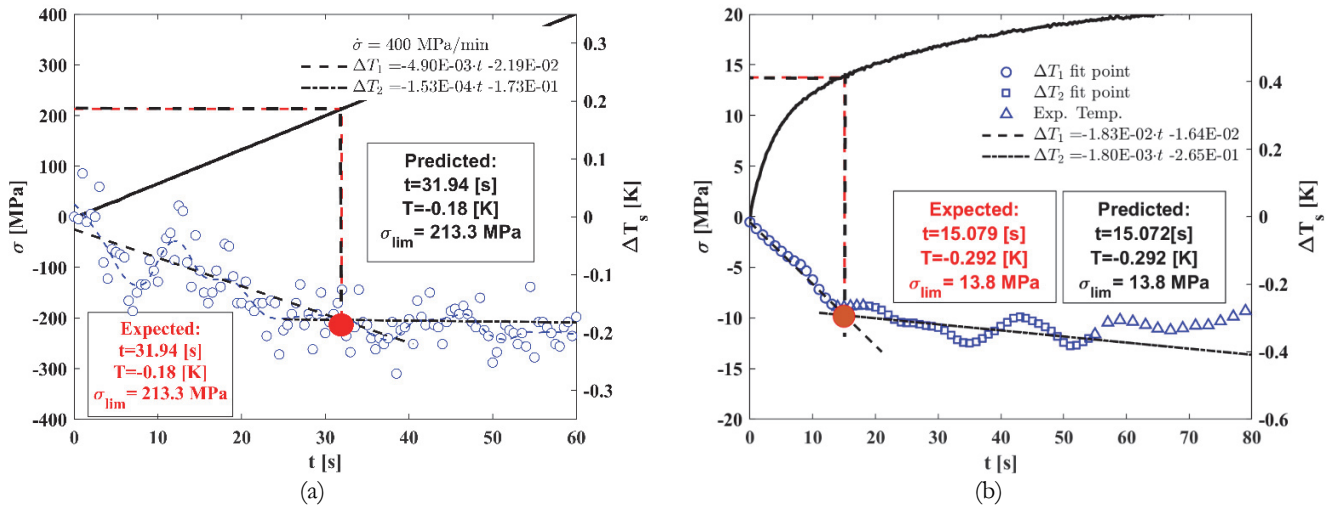

Figure 9: a) C45 Expected vs Predicted limit stress (training); b) PE100 Expected vs Predicted limit stress (training).

Fig. 9 shows how, on a set of data used to train the network, the estimated percentage error on the temperature calculation is 0.01%. The prediction performed on the time values reports a percentage error equal to 0.04%. All this is equivalent to saying that the input data link with the network, i.e., the algorithm can predict the phenomenon's behaviour.
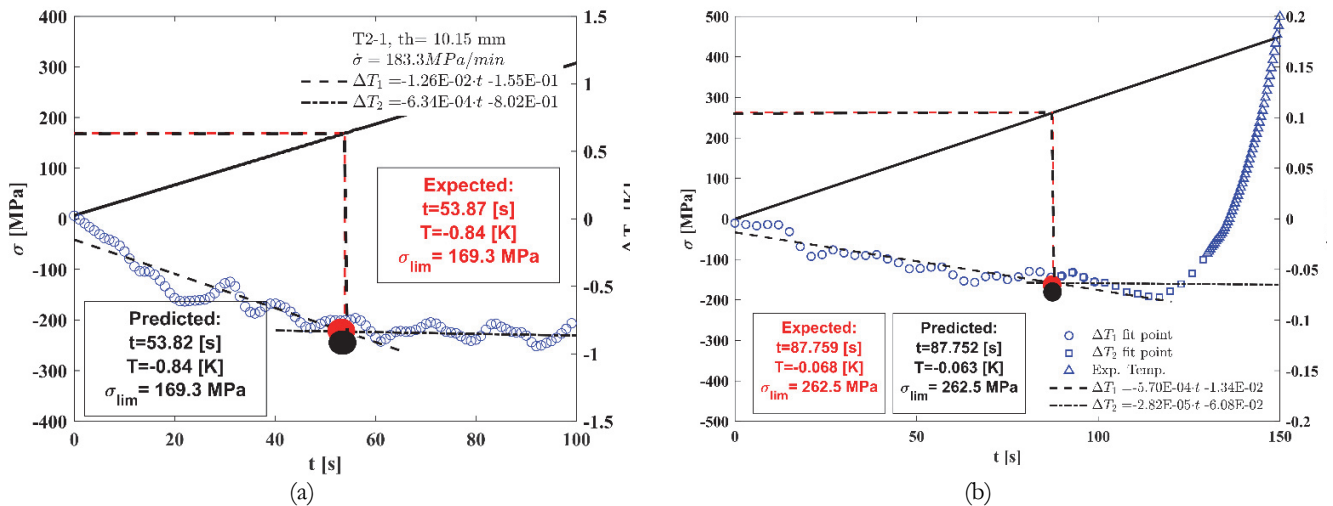

Figure 10: a) S355 Expected vs. Predicted limit stress (test); b) AISI 316L Expected vs. Predicted limit stress (test).

On the other hand, Fig. 10 shows the tests used to validate the accuracy of the algorithm. In this case, it is clear that the estimated percentage error on the temperature calculation is 0.05%, while for time values it is equal to 0.9%. Finally, Fig. 11 represents materials that was not used in the development of the algorithm; therefore, it was not used for training the neural network. In this case, the estimated percent error on the temperature calculation is 0.1%, while for time values the percentage error is equal to 3.3%.

Tab. 1 reports the expected (i.e. assessed by the operator) and the predicted value of the limit stress by the neural network. Each material has been identified according to its use. If it has been used as a training set its identifier is "TRAIN", if it has been a part of the test set its identifier is "TEST". Finally, if it has been used for validation, its identifier is "VALIDATION".
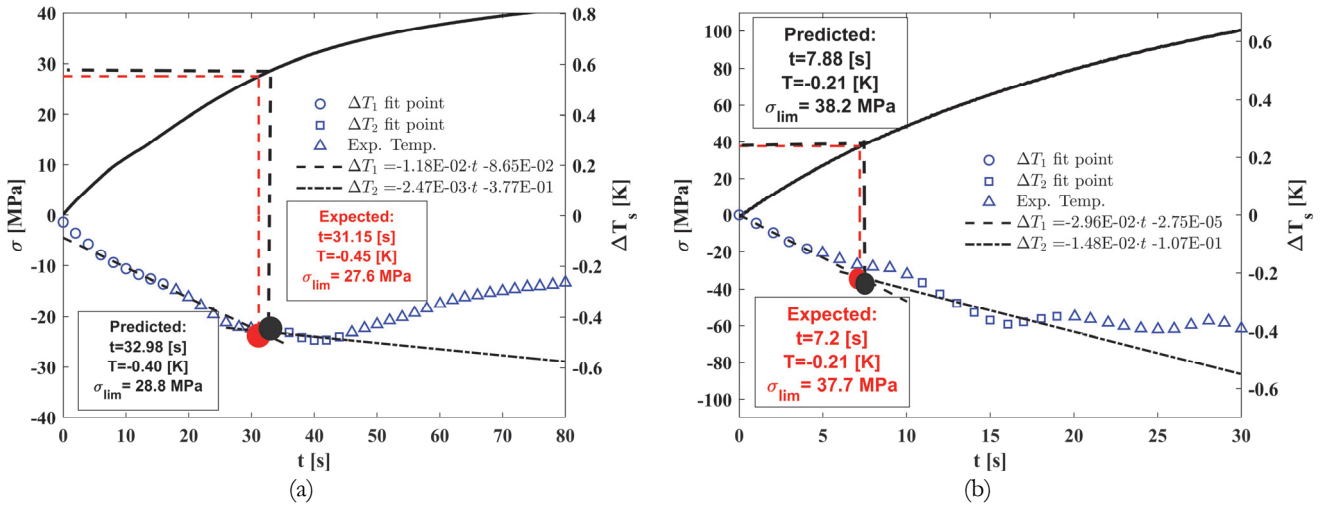

Figure 11: a) PA12 Expected vs. Predicted limit stress (validate); b) PA66GF35 Expected vs. Predicted limit stress (validate).

Material	TEST TYPE	Expected Value			Predicted Value			RMSE		
		t[s]	T[K]	σ_{lim} [MPa]	t[s]	T[K]	σ_{lim} [MPa]	t[s]	T[K]	σ_{lim} [MPa]
PA66GF35 (composites)	TRAINING	8.61	-0.21	38.41	7.88	-0.21	38.95	0.520	0.0001	0.5172
	TRAINING	6.31	-0.28	32.38	7.17	-0.28	32.92	0.600	0.0001	0.6021
	TEST	6.65	-0.34	31.50	7.13	-0.34	32.04	0.330	0.0001	0.3345
	VALIDATION	7.20	-0.21	37.66	7.88	-0.21	38.20	0.480	0.0007	0.4785
	VALIDATION	8.49	-0.25	38.45	7.62	-0.26	38.21	0.620	0.0007	0.6199
AISI316L (steel)	TRAINING	93.27	-0.30	279.96	93.35	-0.30	280.02	0.050	0.0011	0.0554
	TEST	87.57	-0.06	262.45	87.60	-0.07	262.47	0.020	0.0036	0.0176
	VALIDATION	98.09	-0.14	294.49	97.21	-0.14	295.11	0.620	0.0001	0.6218
C45 (steel)	TRAINING	31.94	-0.18	213.32	31.93	-0.18	213.32	0.002	0.0001	0.0029
S355 (steel)	TEST	53.87	-0.84	169.32	53.82	-0.84	169.35	0.030	0.0005	0.033
	TEST	62.17	-0.78	192.96	62.12	-0.78	193.00	0.040	0.0005	0.0406
PA12 (plastic)	TRAINING	36.26	-0.81	29.82	36.26	-0.81	29.82	0.005	0.00003	0.0005
	TEST	40.19	-0.70	30.66	40.19	-0.70	30.66	0.001	0.00001	0.0017
	VALIDATION	31.15	-0.45	27.56	32.98	-0.40	28.85	1.294	0.0353	0.9121
PE100 (plastic)	TRAINING	15.08	-0.29	13.75	15.07	-0.29	13.75	0.005	0.00004	0.0045
	VALIDATION	32.99	-0.93	13.84	34.48	-0.86	14.65	1.053	0.04949	0.5727

Table 1: Comparison of expected vs. predicted values of the limit stress for several kind of material.

The trained network is able to predict the transition temperature at which the first damage occurs. As can be seen from Tab. 1, regarding the predictions made by the neural network, a maximum of 1.2 s of difference between the obtained value and the predicted value can be attested on the entire data set (PA12 tensile tests). As far as the temperature is concerned, a value of 0.049 K (PE100) is attested as the difference between the value obtained and the predicted value. Finally, with

regard to the stress, a value of 0.91 MPa (PA12) is attested as the difference between the value obtained and the predicted value.

CONCLUSIONS

The adoption of the Static Thermographic Method could be useful to identify, with a rapid test procedure, the onset of irreversible micro damage within the material. The transition between the first linear thermoelastic phase and the second temperature decrement phase during a static tensile test can be associated to a macroscopic stress, the limit stress, that applied in a cyclic way can led to the fatigue failure of a structure. However, the assessment of this stress level is up to the operator's experience. In the present work, Neural Network has been trained with a set of experimental data to predict the limit stress according to the observation of the operator. The main outcomes of the study are the following:

- The trained Neural Network returns acceptable results even with a small set of data.
- The predicted limit stress is in good agreement for different class of materials (steels, plastics and composite materials).

Deep Learning algorithms can perform good estimation of the limit stress allowing to automate the procedure to identify it. Future development of the present work will be to expand the adopted dataset, increasing the number of materials, in order to generalize the solutions obtained and overcome the problem of overfitting.

ACKNOWLEDGEMENTS

REFERENCES

[1] Risitano, A., Risitano, G. (2010). Cumulative damage evaluation of steel using infrared thermography, Theor. Appl. Fract. Mech., 54(2), pp. 82–90, DOI: 10.1016/J.TAFMEC.2010.10.002.

[2] Corigliano, P., Cucinotta, F., Guglielmino, E., Risitano, G., Santonocito, D. (2020). Fatigue assessment of a marine structural steel and comparison with Thermographic Method and Static Thermographic Method, Fatigue Fract. Eng. Mater. Struct., 43(4), pp. 734–743, DOI: 10.1111/ffe.13158.

[3] Cucinotta, F., D'Aveni, A., Guglielmino, E., Risitano, A., Risitano, G., Santonocito, D. (2021). Thermal Emission analysis to predict damage in specimens of High Strength Concrete, Frat. Ed Integrità Strutt., 15(55), pp. 258–270, DOI: 10.3221/IGF-ESIS.55.19.

[4] Meneghetti, G., Ricotta, M., Atzori, B. (2016). A two-parameter, heat energy-based approach to analyse the mean stress influence on axial fatigue behaviour of plain steel specimens, Int. J. Fatigue, 82, pp. 60–70, DOI: 10.1016/J.IJFATIGUE.2015.07.028.

[5] Ricotta, M., Meneghetti, G., Atzori, B., Risitano, G., Risitano, A. (2019). Comparison of Experimental Thermal Methods for the Fatigue Limit Evaluation of a Stainless Steel, Met., 9(6), pp. 677, DOI: 10.3390/MET9060677.

[6] Meneghetti, G. (2007). Analysis of the fatigue strength of a stainless steel based on the energy dissipation, Int. J. Fatigue, 29(1), pp. 81–94, DOI: 10.1016/J.IJFATIGUE.2006.02.043.

[7] Geraci, A., La Rosa, G., Risitano, A. (1984).L'infrarosso termico nelle applicazioni meccaniche. CRES Symposium, Catania Italy, pp. 8–9.

[8] La Rosa, G., Risitano, A. (2000). Thermographic methodology for rapid determination of the fatigue limit of materials and mechanical components, Int. J. Fatigue, 22(1), pp. 65–73, DOI: 10.1016/S0142-1123(99)00088-2.

[9] Fargione, G., Geraci, A., La Rosa, G., Risitano, A. (2002). Rapid determination of the fatigue curve by the thermographic method, Int. J. Fatigue, 24(1), pp. 11–19, DOI: 10.1016/S0142-1123(01)00107-4.

[10] Clienti, C., Fargione, G., La Rosa, G., Risitano, A., Risitano, G. (2010). A first approach to the analysis of fatigue parameters by thermal variations in static tests on plastics, Eng. Fract. Mech., 77(11), pp. 2158–2167, DOI: 10.1016/J.ENGFRACMECH.2010.04.028.

[11] Risitano, A., Risitano, G. (2013). Cumulative damage evaluation in multiple cycle fatigue tests taking into account energy parameters, Int. J. Fatigue, 48, pp. 214–222, DOI: 10.1016/j.ijfatigue.2012.10.020.

[12] Risitano, G. (2022). Fatigue strength evaluation of PPGF35 by energy approach during mechanical tests, Frat. Ed Integrità Strutt., 16(59), pp. 537–48, DOI: 10.3221/IGF-ESIS.59.35.

[13] Foti, P., Santonocito, D., Ferro, P., Risitano, G., Berto, F. (2020). Determination of Fatigue Limit by Static Thermographic Method and Classic Thermographic Method on Notched Specimens, Procedia Struct. Integr., 26, pp. 166–174, DOI: 10.1016/J.PROSTR.2020.06.020.

[14] Zhou, K., Wang, W., Huang, L., Liu, B. (2021). Comparative study on the time series forecasting of web traffic based on statistical model and Generative Adversarial model, Knowledge-Based Syst., 213, pp. 106467, DOI: 10.1016/J.KNOSYS.2020.106467.

[15] Crutchfield, J.P. (2012). Between order and chaos, Nat. Phys., DOI: 10.1038/nphys2190.

[16] Curti, G., La Rosa, G., Orlando, M., Risitano, A. (1986). Analisi tramite infrarosso termico della temperatura limite in prove di fatica, Proc. XIV Convegno Naz. AIAS, pp. 211–20.

[17] Thomson, W. (1853). XV. On the Dynamical Theory of Heat, with numerical results deduced from Mr Joule's Equivalent of a Thermal Unit, and M. Regnault's Observations on Steam, Trans. R. Soc. Edinburgh, 20(2), pp. 261–88, DOI: 10.1017/S0080456800033172.

[18] Melvin, A.D., Lucia, A.C., Solomos, G.P., Volta, G., Emmony, D. (1990). Thermal emission measurements from creep damaged specimens of AISI 316L and Alloy 800H, Proc. 9th Int. Conf. Exp. Mech. 2, pp. 765–73.

[19] Melvin, A.D., Lucia, A.C., Solomos, G.P. (1993). The thermal response to deformation to fracture of a carbon/epoxy composite laminate, Compos. Sci. Technol., 46(4), pp. 345–51, DOI: 10.1016/0266-3538(93)90180-O.

[20] Sherstinsky, A. (2020). Fundamentals of Recurrent Neural Network (RNN) and Long Short-Term Memory (LSTM) network, Phys. D Nonlinear Phenom., 404, pp. 132306, DOI: 10.1016/J.PHYSD.2019.132306.

[21] Samih, Y., Maharjan, S., Attia, M., Kallmeyer, L., Solorio, T. (2016). Multilingual Code-switching Identification via LSTM Recurrent Neural Networks, , pp. 50–59, DOI: 10.18653/V1/W16-5806.

[22] Graves, A., Mohamed, A.R., Hinton, G. (2013).Speech recognition with deep recurrent neural networks. ICASSP, IEEE International Conference on Acoustics, Speech and Signal Processing - Proceedings.

[23] Risitano, G., Santonocito, D. (2020). Experimental and numerical assessment of the end of the thermoelastic effect during static traction test, Procedia Struct. Integr., 28, pp. 1449–1457, DOI: 10.1016/j.prostr.2020.10.118.

[24] Santonocito, D. (2021). Numerical and experimental evaluation of the energetic release during static tensile tests on short fiber reinforced composite material, IOP Conf. Ser. Mater. Sci. Eng., 1038(1), pp. 012059, DOI: 10.1088/1757-899X/1038/1/012059.

[25] Santonocito, D. (2020). Evaluation of fatigue properties of 3D-printed Polyamide-12 by means of energy approach during tensile tests, Procedia Struct. Integr., 25, pp. 355–363, DOI: 10.1016/J.PROSTR.2020.04.040.

[26] Risitano, G., Guglielmino, E., Santonocito, D. (2018).Evaluation of mechanical properties of polyethylene for pipes by energy approach during tensile and fatigue tests. Procedia Structural Integrity, 13, pp. 1663–1669.

[27] Gers, F.A., Eck, D., Schmidhuber, J. (2002). Applying LSTM to Time Series Predictable Through Time-Window Approaches, pp. 193–200, DOI: 10.1007/978-1-4471-0219-9_20.